HMGB-1/RAGE signaling inhibition by dioscin attenuates hippocampal neuron damage induced by oxygen-glucose deprivation/reperfusion

AIJUN LIU[1,2*], WENQIAN ZHANG[1,2*], SHUWEI WANG[1,2], YUAN WANG[1,2] and JUN HONG[1,2]

[1]Department of Neurosurgery, Tangshan Gongren Hospital; [2]Department of Brain Trauma, Hebei Institute of Head Trauma, Tangshan, Hebei 063000, P.R. China

Received March 17, 2020; Accepted August 21, 2020

DOI: 10.3892/etm.2020.9361

Abstract. Cerebral ischemia is one of the most common clinical diseases characterized by high morbidity and mortality. Neurocyte apoptosis and a cascade of inflammatory signals following cerebral ischemia-reperfusion injury (IRI) may contribute to secondary brain damage, resulting in severe neurological damage. It has been reported that dioscin, a natural steroid saponin, exerts anti-inflammatory properties against different diseases. The present study aimed to investigate the role of dioscin in oxygen-glucose deprivation/reperfusion (OGD/R) induction in hippocampal cells *in vitro* and *in vivo*. For the *in vitro* study, hippocampal cells were collected from rat embryos of gestational age of E18. The oxygen-glucose deprivation model in primary hippocampal neurons was used to mimic cerebral IRI *in vitro*. To select the optimum dioscin concentration and acting time, cell viability was evaluated by a Cell Counting Kit-8 (CCK-8) assay. Neurons subjected to OGD/R were treated with dioscin and the inflammatory cytokines, high mobility group box chromosomal protein 1 (HMGB-1)/receptor for advanced glycation end products (RAGE) signaling molecules and apoptosis-associated genes were determined. The intracellular reactive oxygen species (ROS) generation was detected. Furthermore, the effects of dioscin on the antioxidant defense mechanisms were evaluated by measuring the activity of glutathione peroxidase (GPx), superoxide dismutase (SOD), catalase (CAT) and the glutathione (GSH)/glutathione disulphide (GSSG) ratio. In addition, OGD/R-induced cells were transfected with pcDNA3.1-HMGB-1 and treated with dioscin, and the neuronal cell apoptosis rate was determined using a terminal deoxynucleotidyl transferase-mediated 2-deoxyuridine 5-triphosphate-biotin nick-end labeling (TUNEL) assay. The mRNA and protein expression levels of the inflammatory factors were measured using real-time quantitative polymerase chain reaction (RT-qPCR) and western blot analysis, respectively. For the *in vivo* investigation, the oxidation and anti-oxidation system in rat hippocampal tissue was evaluated by detecting the expression of the aforementioned oxidative stress-associated proteins, 3-NT as well as 8-oxo-deoxyguanosine (8-OHdG). In the hippocampal region, the apoptotic rate was determined using a TUNEL assay. The results demonstrated that dioscin at a dose of 400 ng/ml significantly reversed the increase in the expression levels of the inflammatory factors and attenuated those of apoptotic cytokines induced by OGD/R. Additionally, dioscin notably reversed the OGD/R-mediated activation of the HMGB-1/RAGE signaling pathway *in vitro* and *in vivo*. Cell treatment with dioscin significantly attenuated ROS production and increased the activity of antioxidant enzymes. Additionally, increasing the expression of HMGB-1 inhibited the protective effects of dioscin on cell apoptosis in the OGD/R-induced neurons. Furthermore, HMGB-1 overexpression reversed the antiapoptotic and anti-inflammatory effects of dioscin on neurons. The results of the present study indicated that dioscin exerted anti-inflammatory, antiapoptotic and antioxidant effects via the HMGB-1/RAGE signaling pathway. These results suggest a novel perspective of the protective effects of dioscin as a prospective remedial factor for IRI.

Correspondence to: Professor Jun Hong, Department of Neurosurgery, Tangshan Gongren Hospital, 27 Wenhua Road, Tangshan, Hebei 063000, P.R. China
E-mail: 2633955818@qq.com

*Contributed equally

Key words: dioscin, oxygen-glucose deprivation, inflammation, apoptosis, high mobility group box-1 protein

Introduction

Ischemic stroke is widely recognized as a severe cerebrovascular disease with high mortality and morbidity rates (1), caused by arterial inflow interruption and nutrient and oxygen deficits. Timely restoration of cerebral blood flow perfusion in the ischemic area is pivotal to minimize sustained brain injury. However, reperfusion following a period of ischemia may lead to cerebral ischemia-reperfusion injury (IRI). Furthermore, restored blood supply may trigger the production of excessive amounts of reactive oxygen species (ROS), oxidative stress-related factors (2), and inflammatory responses (3).

Therefore, inflammation modulators and ROS scavengers may serve as a promising treatment approach for IRI.

In the inflammatory network, high mobility group box chromosomal protein 1 (HMGB-1) is a potent inflammatory cytokine, which activates the downstream inflammatory signaling pathway (4). A previous study has demonstrated that dynamic changes in the serum HMGB-1 levels are associated with inflammatory responses following cardiopulmonary bypass (5). Therefore, HMGB-1 levels are considered as a monitoring marker of inflammation during cardiac surgery with cardiopulmonary bypass (5). Although a limited number of studies have been conducted regarding the association between HMGB-1 and cerebral IRI, HMGB-1 is hypothesized to serve an important role in multiple-organ IRI through protecting against hepatic injury following murine liver ischemia-reperfusion (6). As a ligand with high affinity to HMGB-1, the receptor for advanced glycation end products (RAGE) is able to specifically combine with HMGB-1, participating in the inflammatory response in the late stages of sepsis (7). In addition, HMBG-1/RAGE axis may serve a significant role in the development of chronic inflammatory diseases such as neutrophilic asthma (8). Therefore, the present study hypothesized that the inhibition of the HMBG-1/RAGE signaling pathway may attenuate inflammatory responses, indicating a possible neuroprotective effect in cerebral IRI.

Dioscin, a highly fat-soluble steroidal saponin, is present in a number of plants such as ginseng (9) and *Dioscorea nipponica* Makino (10). Modern pharmacological studies have suggested that dioscin exerts anti-inflammatory effects via alleviating the lipopolysaccharide-induced inflammatory kidney injury (11). Previous studies have revealed that dioscin not only has significant effects on the anti-inflammatory responses, but also exhibits antiviral (12), antioxidative (13), hepatoprotective (14) and antiapoptotic activities (15). Furthermore, numerous studies have focused on the neuroprotective effects of dioscin following peripheral and central nerve injury (16-19). However, there is little information available regarding the potential mechanisms of dioscin on inducing cerebral IRI. Whether dioscin mediates its beneficial effects through a combination of multiple mechanisms or a single pathway, or by an anti-inflammatory mechanism, remains largely unknown. Therefore, the present study aimed to assess whether the therapeutic effects of dioscin on cerebral IRI were associated with its anti-inflammatory or other medicinal properties, and to further investigate the role of the HMGB-1/RAGE signaling pathway in these mechanisms.

Materials and methods

Cell culture. Primary hippocampal neuronal cultures were prepared as previously described (20). Briefly, following harvesting the Sprague-Dawley (SD) rat embryos at embryonic day 18 (E18), hippocampi were chopped and digested with 0.25% trypsin at 37˚C for 15 min. Animal experiments were approved by the Animal Care and Use Committee of the Tangshan Gongren Hospital (Tangshan, China; approval no. GRYY-LL-2019-15). All animal experimental procedures were performed according to the National Institutes of Health Guide for the Care and Use of Laboratory Animals (NIH Publication no. 85-23, revised 1996) (21). Following filtration, cells were seeded at a density of $3x10^5$ cells/well onto 12-well plates. Neurons were maintained at 37˚C in a neurobasal medium (Invitrogen; Thermo Fisher Scientific, Inc.) supplemented with 2% B-27 and 0.5 mM glutamine (both from Invitrogen; Thermo Fisher Scientific, Inc.) and half of the cell-culture medium was replaced every 3 days.

OGD/R model. To mimic cerebral IRI *in vitro*, an OGD/R model was established as previously described (22). Briefly, primary hippocampal neurons were cultured from E18 SD rats as aforementioned. Neurons were maintained in glucose-free DMEM (cat. no. 11966-025; Gibco; Thermo Fisher Scientific, Inc.) and cultured in an O_2-free chamber at 37˚C for 2 h. During the reoxygenation process, the cell-culture medium was replaced with normal DMEM, and neurons were then cultured in an incubator under normoxic conditions at 37˚C and 5% CO_2 for an additional 12 h. Control cells were treated in the same conditions without being exposed to OGD/R.

Drug administration. Dioscin was obtained from Sigma-Aldrich; Merck KGaA (cat. no. SMB00576), and dissolved in dimethyl sulfoxide (DMSO), at a final concentration of DMSO <0.1%. Neurons were then divided into the following four groups: i) Control group, where neurons were not treated; ii) Control + dioscin group, where primary hippocampal neurons were treated with dioscin without OGD/R; iii) OGD/R group, where primary hippocampal neurons subjected to OGD/R; and iv) the OGD/R + dioscin group, where primary neurons subjected to reoxygenation following oxygen-glucose deprivation. The optimum concentration and action time of dioscin treatment was determined using Cell Counting Kit-8 (CCK-8) assay.

CCK-8 assay. The viability of neurons was assessed by a CCK-8 assay (MedChemExpress). For CCK-8 analysis, cells were plated into 96-well plates at a density of $5x10^3$ cells/well for 24 h at 37˚C with 5% CO_2. Subsequently, cells were subjected to OGD for 2 h and reperfusion for 12 h, and then different concentrations of dioscin (0, 100, 200, 400 and 800 ng/ml) were added to the culture medium for a 24-h intervention period. A total of 10 μl CCK-8 solution was carefully added to the culture medium, and cells were incubated for an additional 2 h at 37˚C, according to the manufacturer's instructions. Finally, cell viability was determined by measuring the absorbance at a wavelength of 570 nm using a microplate reader.

Western blot analysis. Neurons were collected, lysed in radioimmunoprecipitation assay (RIPA) lysis buffer, centrifuged at 12,000 x g at 4˚C for 15 min and the concentration of the extracted proteins was determined using the bicinchoninic acid Protein Assay kit (Beyotime Institute of Biotechnology). A total of 25 μg protein was then separated by SDS-PAGE and electro-transferred onto nitrocellulose membranes using a Bio-Rad mini-protein-III wet transfer unit (Bio-Rad Laboratories, Inc.) at 90 V/90 min. Following blocking with non-fat milk for 2 h at room temperature, membranes were incubated with primary antibodies at 4˚C overnight. The primary antibodies used were against β-actin (cat. no. sc-47778; 1:1,000, mouse; Santa Cruz Biotechnology, Inc.), interleukin (IL)-1 (cat. no. sc-7884; 1:1,000, rabbit; Santa Cruz Biotechnology, Inc.), IL-6 (cat. no. sc-7920; 1:1,000, rabbit; Santa Cruz Biotechnology, Inc.), tumor necrosis factor α (TNF-α;

cat. no. sc-52746; 1:1,000, mouse; Santa Cruz Biotechnology, Inc.), HMGB-1 (cat. no. 6893; 1:1,000, rabbit; Cell Signaling Technology, Inc.), RAGE (cat. no. sc-5563; 1:1,000, rabbit; Santa Cruz Biotechnology, Inc.), Bax (cat. no. 2772; 1:1,000, rabbit; Cell Signaling Technology, Inc.), Bcl-2 (cat. no. sc-7382; 1:1,000, mouse; Santa Cruz Biotechnology, Inc.), 3-NT (cat. no. ab61392; 1:1,000, mouse; Abcam) and cleaved caspase-3 (cat. No. 9661; 1:1,000; rabbit; Cell Signaling Technology, Inc.). Following washing with PBS 3 times, membranes were incubated with horseradish peroxidase (HRP) conjugated anti-rabbit IgG and anti-mouse IgG (cat. nos. sc-2357 and sc-516102, 1:2,000; Santa Cruz Biotechnology, Inc.) for 1.5 h at room temperature. Finally, the protein density was measured using a Bio-Rad imaging system and analyzed with the ImageJ software (Image Lab 4.1; National Institutes of Health). Relative protein expression levels are presented as the densitometric value (OD values) ratio of the target protein band to β-actin band.

Reverse transcription-quantitative (RT-q)PCR analysis. Total cellular RNA was isolated with the TRIzol® reagent (Invitrogen; Thermo Fisher Scientific, Inc.), according to the manufacturer's protocol. Subsequently, RNA concentration was measured using a UV spectrophotometer (NanoDrop One Microvolume UV-Vis spectrophotometer; Thermo Fisher Scientific, Inc.) and the RT assay was performed, using RNA as template, with PrimeScript™ RT reagent kit (cat. no. RR037A; Takara Bio, Inc.) to synthesize cDNA. The RT reactions were performed at 37˚C for 15 min, 85˚C for 5 sec and 4˚C for cooling. In total, 2 μg RNA from each sample were reverse transcribed into cDNA. The RT-qPCR was conducted with the TB Green® Premix Ex Taq™ II kit (cat. no. RR820A; Takara Bio, Inc.) in a 20 μl reaction containing 10 μl 2X TB Green Premix Ex Taq II (Tli RNaseH Plus), 0.8 μl forward primer (10 μM), 0.8 μl reverse primer (10 μM), 2 μl template DNA and 6.4 μl ddH_2O. The thermocycling conditions of the qPCR were as follows: 37˚C for 30 min, 95˚C for 55 sec to inactivate reverse transcriptase, followed by 40 cycles of two-step PCR, 95˚C for 20 sec and 60˚C for 50 sec. The final extension was performed at 75˚C for 10 min and samples were subsequently held at 4˚C. A total of 3 independent experiments were performed for each group. The primer sequences used in this study were the following: For β-actin, forward 5'-TGACGT GGACATCCGCAAAG-3' and reverse, 5'-CTGGAAGGT GGACAGCGAGG-3'; IL-1β, forward 5'-TGGGAGATGGAA ACATCCAG-3' and reverse, 5'-GCATTTTACTGACTGCAC GG-3'; IL-6, forward 5'-ACAGCCACTCACCTCTTCAG-3' and reverse, 5'-CCATCTTTTTCAGCCATCTTT-3'; TNF-a, forward 5'-AGAACCCCCTGGAGATAACC-3' and reverse, 5'-AAGTGCAGCAGGCAGAAGAG-3'; HMGB-1, forward 5'-GCAGATGACAAGCAGCCTTA-3' and reverse, 5'-TTT GCTGCATCAGGCTTTCC-3'; RAGE, forward 5'-GACTCT TAGCTGGCACTTGGAT-3' and reverse, 5'-GGACTTCAC AGGTCAGGGTTAC-3'; cleaved caspase-3, forward 5'-AGC AATAAATGAATGGGCTGAG-3' and reverse, 5'-GTATGG AGAAATGGGCTGTAGG-3'; Bax, forward 5'-GTTGCC CTCTTCTACTTTGC-3' and reverse, 5'-ATGGTCACTGTC TGCCATG-3'; and Bcl-2 forward, 5'-GGTCCTCCAGTGGGT ATTT-3' and reverse, 5'-TCCTCCTGAGACTGCCTTAT-3'. β-actin was used as an internal control and the $2^{-\Delta\Delta Cq}$ method was applied to determine the relative gene expression (23).

Intracellular ROS detection. For the detection of intracellular ROS, the Reactive Oxygen Species Assay kit was applied, according to the manufacturer's instructions (cat. no. ab113851; Abcam). Following treatment with and without OGD/R, dioscin or under control conditions for 24 h, 2',7'-dichlorofluorescein diacetate (DCFH-DA; concentration, 5 μmol/l) was added in the culture medium. The cell mixture was then incubated at 37˚C in a 5% CO_2 incubator for 30 min for the conversion of DCFH-DA to 2',7'-dichlorofluorescein. Subsequently, cells were fixed with 1% paraformaldehyde for 10 min at 4˚C and the levels of intracellular ROS were determined using the cellular ROS detection assay kit with flow cytometry (BD Accuri™ C6; BD Bioscience). Finally, the results were analyzed using the FlowJo software version 7.6.5 (FlowJo, LLC).

Determination of the glutathione (GSH)/glutathione disulfide (GSSG) ratio. The effects of dioscin on non-enzymatic antioxidant defense mechanisms were evaluated by detecting the GSH and GSSG levels in neurons, according to the method proposed by Hissin and Hilf (24), with slight modifications. A proprietary non-fluorescent dye thiol green indicator was used in the GSH/GSSG assay protocol, but without O-phthalaldehyde as the fluorescent reagent. The concentration of GSH and GSSG were measured using the GSH/GSSG Ratio Detection Assay kit (cat. no., ab138881; Abcam). The levels of GSH (reduced form) and total GSH (GSH + GSSG) were directly measured using their standards provided by the kit. Then, the GSSG content was indirectly determined by calculating the difference between total GSH + GSSG and GSH. Finally, the GSH/GSSG ratio was calculated.

Measurement of glutathione peroxidase (GPx), catalase (CAT) and superoxide dismutase (SOD) activity. The effects of dioscin on the enzymatic antioxidant defense mechanisms were determined by measuring the GPx, CAT and SOD activity. The activity of GPx was spectrophotometrically detected in neurons as previously described (25). The GPx activity was expressed as the amount of the oxidized NADPH protein in min/mg and the activity rate was determined by the change in absorbance at 340 nm (A340). When the substrate tert-butyl hydroperoxide was added, the reaction was initiated and the reduction in GPx activity was recorded at A340. Additionally, GPx activity was expressed in nmol/min/mg of protein. Furthermore, CAT activity was assayed as previously described (26), using H_2O_2 as the substrate. The decomposition of H_2O_2 was determined at 240 nm by measuring the decrease in absorbance. The CAT activity was expressed as μM/min/mg protein. Finally, SOD activity was spectrophotometrically determined in kinetic mode at intervals of 1 min up to 3 min at 560 nm, as described by Hassan *et al* (27). SOD activity was expressed as U/mg of protein.

Cell transfection. For cell transfection, cells were cultured at a density of $1x10^5$ cells/well. Neurons were grown in six-well plates for 24 h and then transfected with the pcDNA3.1-HMGB-1 overexpression plasmid (2 μg) or control vector for 24 h using Lipofectamine® 2000 (Invitrogen; Thermo Fisher Scientific, Inc.) according to the manufacturer's protocol. The pcDNA3.1-HMGB-1 overexpression plasmid was synthesized by Applied Biological Materials, Inc. Neurons transfected with control vector, were considered as the negative control group.

Furthermore, the overexpression of the HMGB-1 was assessed using western blot analysis 6 h post-transfection.

Analysis of neuronal apoptosis by terminal deoxynucleotidyl transferase-mediated (dUTP) nick-end labeling (TUNEL) staining. TUNEL staining was performed to detect cell apoptosis according to the manufacturer's protocol. Briefly, neurons at a density of $5x10^4$ cells/cm^2 were fixed with 4% paraformaldehyde at 4˚C for 20 min. The ischemic brain tissue was embedded in paraffin and sectioned at 5 μm following fixing in 4% paraformaldehyde at room temperature for 48 h. Following dewaxing and rehydration, sections were incubated with a proteinase K solution for 15 min at 37˚C. Subsequently, cells were treated with a green fluorescein-labeled dUTP solution and incubated with 4',6-diamidino-2-phenylindole (DAPI, 1 μg/ml) for 5 min at room temperature to detect cell nuclei. The TUNEL-positive cells and morphology of neurons were observed under a fluorescence microscope and cells were counted in 5 randomly selected microscopic fields (magnification, x200). The cell apoptosis rate was calculated as the number of TUNEL-positive cells/the number of DAPI stained cells.

Animals and middle cerebral artery occlusion (MCAO) model. A total of 50 12 weeks-old adult male SD rats were obtained from the Experimental Animal Center, North China University of Science and Technology. All rats were housed under a controlled environment at 22-24˚C, with a 12/12 h light/dark cycle and 50-55% humidity. All rats were provided with *ad libitum* access to food and water throughout the whole trial. MCAO was used to establish the cerebral IRI rat model. In brief, anesthesia was administered to rats by intraperitoneal injection of 50 mg/kg sodium pentobarbital. Following separation of the carotid arteries including common carotid artery (CCA), internal carotid artery (ICA) and external carotid artery (ECA), the right CCA was carefully ligated with a microclip. Middle cerebral artery (MCA) occlusion was induced by a monofilament inserted into the stump of the ICA, following which the monofilament was advanced to the origin of the MCA to occlude it. A Laser-Doppler flowmeter (Moor Instruments, Ltd.) was used to monitor regional cerebral blood flow (rCBF) of each rat. A 70-80% decrease in rCBF was regarded as successful MCAO. Occlusion was maintained for a period of 60 sec. The monofilament was then removed to reestablish carotid blood flow. Sham-operated rats underwent only the carotid artery separation without the monofilament insertion. A total of rats succumbed during the establishment of the MCAO model.

Experimental groups and treatment. Rats were randomly allocated into the following five groups: Sham; sham + dioscin; MCAO; MCAO + dioscin; and MCAO + dioscin + HMGB-1. Dioscin was suspended in 0.5% sodium carboxyl methyl cellulose solution prior to use. Rats were treated with dioscin (60 mg/kg) by gavage at 1 h following establishment of the MCAO rat model and once daily for the subsequent 6 days. In addition, rats in the sham and MCAO groups were treated with equal volumes of sodium carboxyl methyl cellulose solution. Following treatment with dioscin or sham for 30 min, rats in the MCAO + dioscin + HMGB-1 group were treated with HMGB-1 (50 ug/kg; R&D Systems, Inc.) by intraperitoneal injection once daily for 6 days.

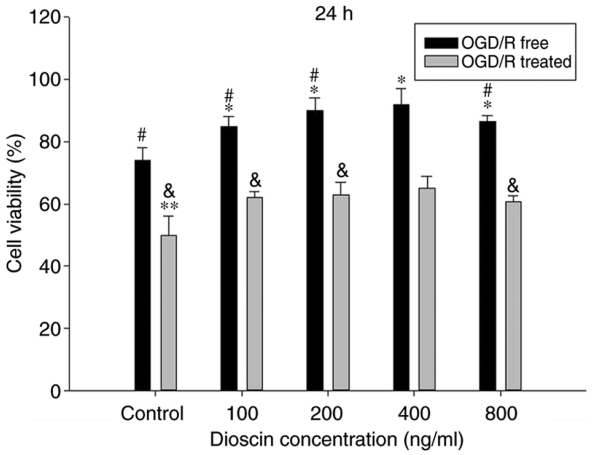

Figure 1. Dioscin affects cell viability of hippocampal neurons. Neurons were treated with different concentrations (100, 200, 400 and 800 ng/ml) of dioscin with or without OGD/R for 24 h. Values are presented as the mean ± standard deviation (SD). *P<0.05 and **P<0.01 compared with the OGD/R-free condition of the control group. $^{\#}$P<0.05 compared with OGD/R-free condition of the dioscin-treated group (400 ng/ml). $^{\&}$P<0.05 compared with the OGD/R condition of the dioscin-treated group (400 ng/ml). OGD/R, oxygen-glucose deprivation/reperfusion.

Detection of 8-oxo-deoxyguanosine (8-OHdG). 8-OHdG is a biomarker of nucleic acid oxidation. Therefore, 8-OHdG was assessed in frozen sections of brain tissue by immunofluorescence. Following treatment with 0.4% Triton X-100 at room temperature for 10 min, sections were incubated with a mixture containing a primary 8-OHdG antibody (cat. no. ab62623, 1:1,000, mouse, Abcam) and a nuclear protein (NeuN, ab104224, 1:1,000, mouse, Abcam) monoclonal antibody at 4˚C overnight. The next day, sections were incubated with HRP-conjugated secondary antibody (cat. no. ab205719, 1:500, Abcam) for 1 h at 37˚C. Chromosomes were counterstained with DAPI (1 μg/ml) for 10 min at room temperature and the fluorescence images were captured using an Olympus F1000 laser scanning confocal fluorescence microscope (magnification, x400; Olympus Corporation).

Statistical analysis. All statistical analyses were performed with the SPSS 23.0 software (SPSS Inc.). All parameters were expressed as the mean ± standard error of the mean (SEM) and were obtained from ≥3 replicates. Data were analyzed using one-way ANOVA followed by Tukey's post hoc analysis. P<0.05 was considered to indicate a statistically significant difference.

Results

Effects of dioscin on OGD/R-induced cell viability. To evaluate the functional effects of dioscin on neurons subjected to OGD/R or not, cells were treated with different doses of dioscin (100, 200, 400 and 800 ng/ml) and cell viability was assessed. OGD/R significantly inhibited cell viability in cells treated with any concentration of dioscin. Compared with the control group, dioscin at 100, 200 and 400 ng/ml markedly promoted neuron viability in cells subjected to OGD/R or not (P<0.05; Fig. 1). However, dioscin at 800 ng/ml markedly inhibited cell viability compared with cells treated with 400 ng/ml

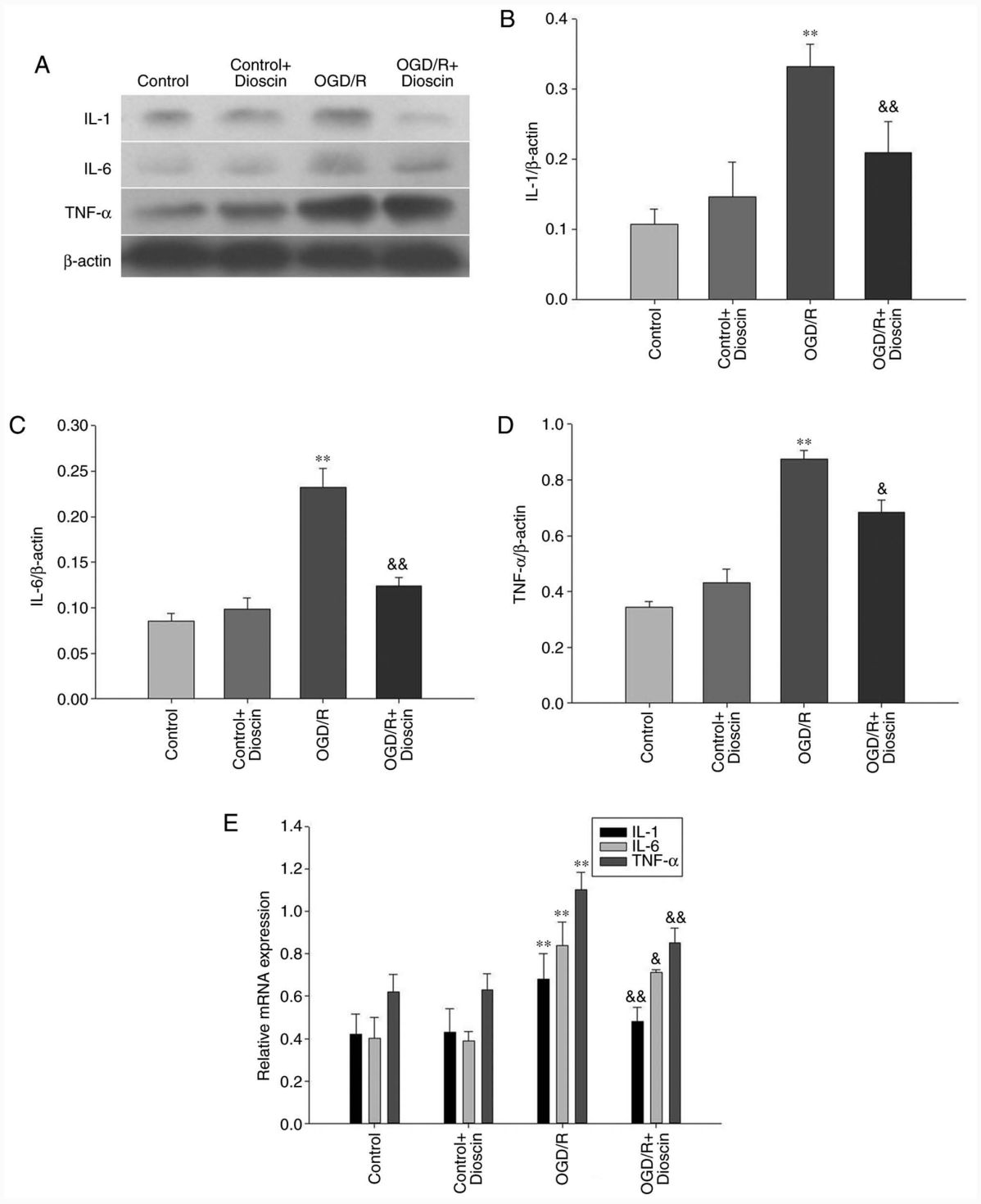

Figure 2. Dioscin downregulates the protein expression levels of IL-1, IL-6 and TNF-α. (A) Representative western blot analysis results showing IL-1, IL-6 and TNF-α expression at 24 h following dioscin treatment. (B) Densitometric quantification of the IL-1/β-actin, (C) IL-6/β-actin and (D) TNF-α/β-actin ratio at 24 h following dioscin treatment. (E) Relative mRNA expression of IL-1, IL-6 and TNF-α at 24 h following dioscin treatment. Values are expressed as the mean ± standard error of the mean (SEM). **P<0.01 vs. the control group. $^{\&}$P<0.05 and $^{\&\&}$P<0.01 vs. the OGD/R group. IL-1, interleukin 1; TNF-α, tumor necrosis factor α; OGD/R, oxygen-glucose deprivation/reperfusion.

dioscin (P<0.05; Fig. 1). Therefore, dioscin at a concentration of 400 ng/ml was used in subsequent experiments.

Dioscin inhibits the protein expression levels of IL-1, IL-6 and TNF-α. IL-1, IL-6 and TNF-α were downregulated in the control group. Following reperfusion, the expression levels of IL-1, IL-6 and TNF-α were significantly increased in the OGD/R group. However, treatment with dioscin restored the OGD/R-mediated overexpression of IL-1, IL-6 and TNF-α (P<0.05; Fig. 2). The same results were also observed in the mRNA level when RT-qPCR was applied (P<0.05; Fig. 2E).

Dioscin inhibits the expression of apoptosis-associated proteins. Cleaved caspase-3 and Bax protein expression

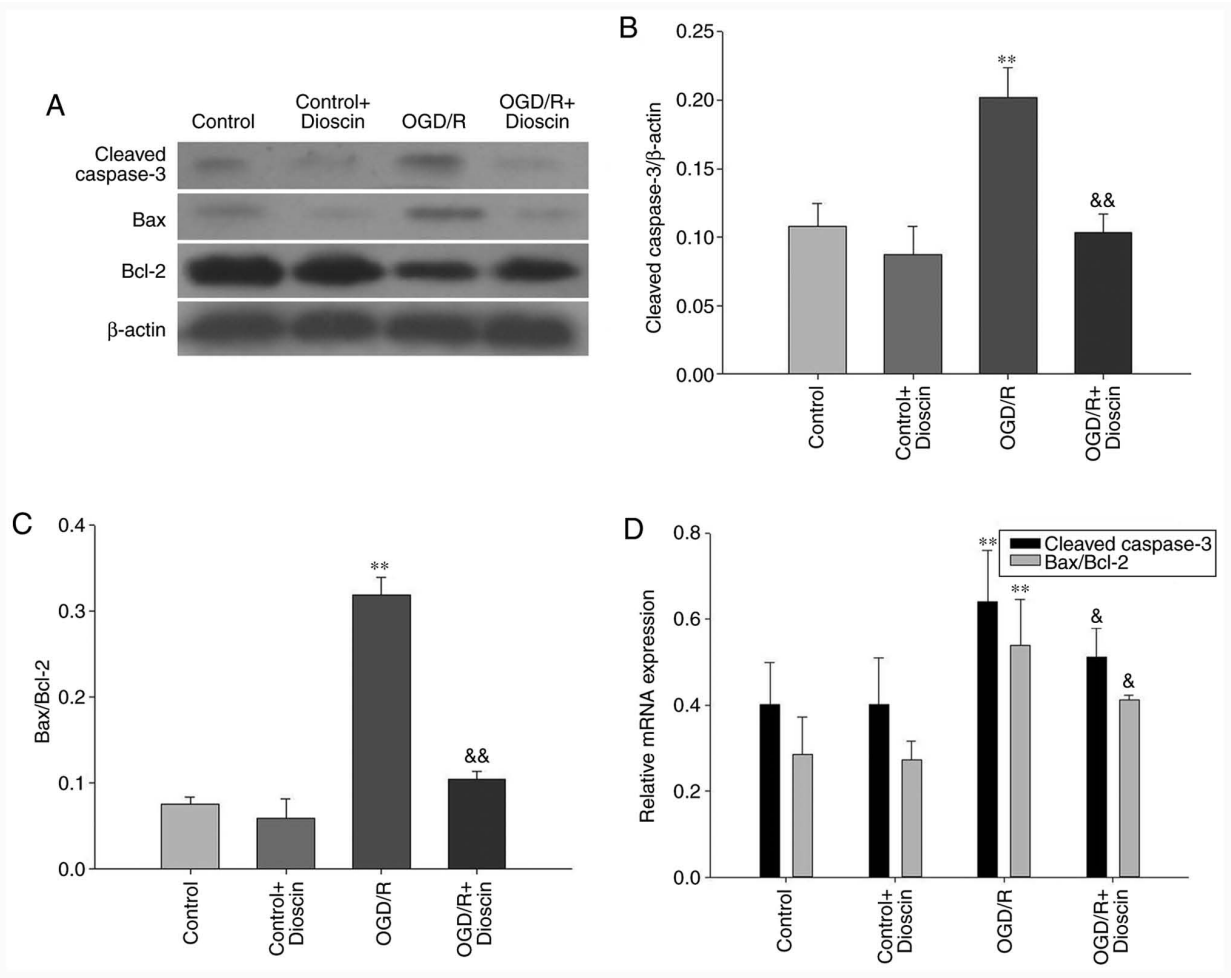

Figure 3. Dioscin treatment inhibits the expression of apoptosis-associated proteins. (A) Representative western blot analysis results indicating the protein expression of cleaved caspase-3, Bax and Bcl-2 at 24 h following dioscin treatment. Densitometric quantification of the (B) cleaved caspase-3/β-actin and (C) Bax/Bcl-2 ratio at 24 h following dioscin treatment. (D) Relative mRNA expression of cleaved caspase-3, Bax and Bcl-2 at 24 h following dioscin treatment. Values are expressed as the mean ± standard error of the mean (SEM). **P<0.01 vs. the control group. $^{\&}$P<0.05 and $^{\&\&}$P<0.01 vs. the OGD/R group. OGD/R, oxygen-glucose deprivation/reperfusion.

levels were decreased in the control groups. Furthermore, the protein and mRNA expression levels of both cleaved caspase-3 and Bax were markedly increased, and those of Bcl-2 were decreased in the OGD/R group. However, cell treatment with dioscin significantly attenuated the expression levels of cleaved caspase-3 and Bax. In the OGD/R + dioscin group, the mRNA and protein expression levels of Bcl-2 were notably increased compared with those in the OGD/R group (P<0.05; Fig. 3).

Dioscin inhibits the OGD/R-induced activation of the HMGB-1/RAGE pathway. The results demonstrated that the expression levels of HMGB-1 and RAGE were significantly elevated in the OGD/R group. However, following treatment with dioscin, the expression of proteins involved in the HMGB-1/RAGE pathway was downregulated (OGD/R + dioscin group; P<0.05; Fig. 4A and B). The expression levels of HMGB-1/RAGE at the mRNA level, detected by RT-qPCR, were consistent with those observed at the protein level (Fig. 4C).

Dioscin markedly decreases ROS production and promotes the antioxidant defense system. Compared with the control group, intracellular ROS production in the neurons was significantly increased in the OGD/R group (P<0.01). Additionally, dioscin treatment in the OGD/R + dioscin group significantly inhibited ROS production compared with the OGD/R group (P<0.05; Fig. 5A). Furthermore, to evaluate the antioxidant defense system, the levels of the antioxidant enzymes, GPx, CAT and SOD, and the ratio of the non-enzymatic antioxidants GSH/GSSG were measured. The results indicated that the levels of GPx, CAT, SOD and the GSH/GSSG ratio were decreased in neurons subjected to OGD/R compared with those noted to the control group (P<0.05; Fig. 5). Nevertheless, co-treatment of OGD/R-treated neurons with dioscin significantly elevated the expression of the antioxidant compounds compared with the OGD/R group (P<0.05).

Upregulation of HMGB-1 with the pcDNA3.1-HMGB-1 plasmid diminishes the protective effects of dioscin on neuron apoptosis. Subsequently, neuronal apoptosis was evaluated using TUNEL/DAPI staining. Therefore, hippocampal neurons were transfected with the pcDNA3.1-HMGB-1 plasmid to overexpress HMGB1. As demonstrated in Fig. 6,

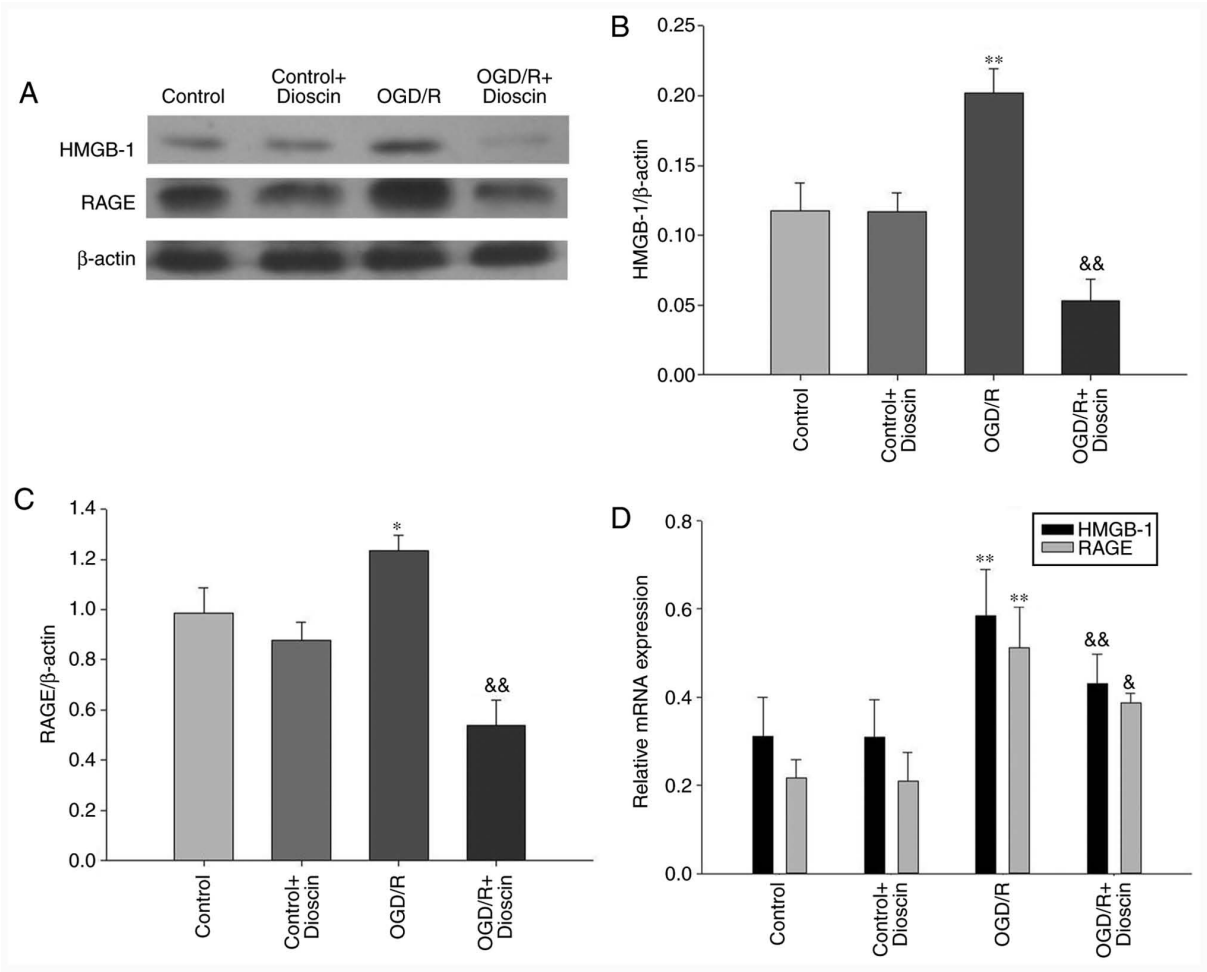

Figure 4. Dioscin inhibits the OGD/R-mediated activation of the HMGB-1/RAGE pathway. (A) Western blot analysis results showing HMGB-1 and RAGE protein expression at 24 h following dioscin treatment. Densitometric quantification of the (B) HMGB-1/β-actin and (C) RAGE/β-actin ratio at 24 h following dioscin treatment. (D) Relative mRNA expression levels of HMGB-1 and RAGE at 24 h following dioscin treatment. Values are expressed as the mean ± standard error of the mean (SEM). *P<0.05 and **P<0.01 vs. the control group. $^{\&}$P<0.05 and $^{\&\&}$P<0.01 vs. the OGD/R group. OGD/R, oxygen-glucose deprivation/reperfusion; HMGB-1, high mobility group box chromosomal protein 1; RAGE, receptor for advanced glycation end products.

the number of TUNEL-positive cells was markedly increased in the OGD/R group. Furthermore, quantitative analysis indicated that dioscin significantly decreased neuronal apoptosis in the OGD/R + dioscin group. Following transfection with pcDNA3.1-HMGB1, the number of TUNEL-positive cells was notably increased (P<0.01; Fig. 6). These results indicated that upregulation of HMGB-1 may inhibit the protective effects of dioscin against OGD/R-induced apoptosis on hippocampal neurons.

HMGB-1 overexpression may offset the suppressive effects of dioscin on proinflammatory cytokine expression. Therefore, compared with the OGD/R + dioscin group, western blot analysis indicated that HMGB-1 overexpression significantly increased the expression of inflammatory cytokines, namely IL-1, IL-6 and TNF-α (P<0.05; Fig. 7A-C).

Activation of the HMGB-1/RAGE pathway may reverse the effect of dioscin on antioxidant stress. The results demonstrated that HMGB-1 overexpression reversed the protective effects of dioscin on ROS generation and the activity of antioxidant enzymes (P<0.05; Fig. 7). Therefore, treatment of neurons with the pcDNA3.1-HMGB-1 plasmid significantly elevated ROS production compared with that observed in the OGD/R + dioscin group (P<0.01; Fig. 7D). Furthermore, compared with the OGD/R group, the activities of GPx, CAT and SOD were increased in the OGD/R + dioscin group, while this effect was restored following HMGB-1 overexpression (P<0.05; Fig. 7E-G). However, there was no marked statistically significant difference in the degradation of GSH/GSSG between the OGD/R + dioscin + pcD NA3.1-HMGB-1 and OGD/R + dioscin groups (P<0.05; Fig. 7H).

Dioscin significantly alleviates oxidative stress and apoptosis of hippocampal neurons in the MCAO model via the HMGB-1/RAGE pathway. The results of the MCAO model demonstrated that intracellular ROS production, and 3-NT and 8-OHdG expression in the neurons were significantly elevated compared with the sham group (P<0.01; Fig. 8A, B and G). By contrast, MCAO significantly attenuated the activity of antioxidant enzymes and non-enzymatic antioxidants compared with the sham group (P<0.01; Fig. 8C-F). Furthermore, dioscin improved the antioxygenic ability following MCAO. However,

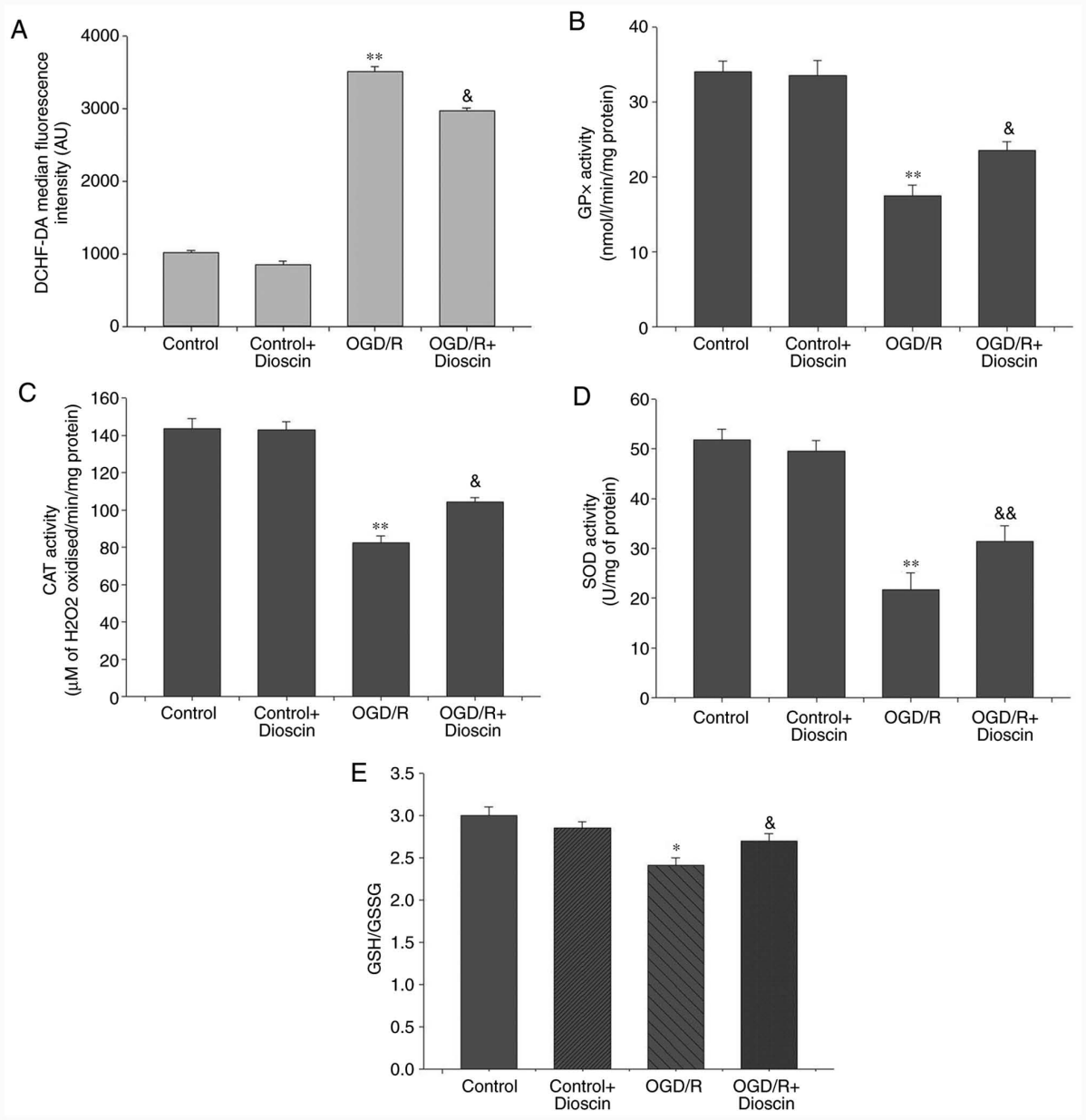

Figure 5. Dioscin remarkably decreases ROS production and promotes the antioxidant defense system. Dioscin inhibited ROS generation in OGD/R-subjected neurons. (A) DCHF-DA fluorescence intensity was quantified by flow cytometry. Dioscin improved the enzymatic antioxidant defense mechanisms in OGD/R-subjected neurons. (B) GPx, (C) CAT and (D) SOD activities were evaluated in cultured primary hippocampal cells. Dioscin improved the non-enzymatic antioxidant defense mechanisms in OGD/R-subjected neurons. (E) GSH/GSSG ratio was evaluated in primary hippocampal cells. Values are expressed as the mean ± standard error of the mean (SEM). *P<0.05 and **P<0.01 vs. the control group. $^{\&}$P<0.05 and $^{\&\&}$P<0.01 vs. the OGD/R group. ROS, reactive oxygen species; OGD/R, oxygen-glucose deprivation/reperfusion; DCHF-DA, 2',7'-dichlorofluorescein diacetate; GPx, glutathione peroxidase; CAT, catalase; SOD, superoxide dismutase; GSH/GSSG, glutathione/glutathione disulphide.

it did not elevate the activity of the non-enzymatic antioxidants through the HMGB-1/RAGE pathway. Additionally, HMGB-1 overexpression reversed the decreased ROS production, and 3-NT and 8-OHdG expression, as well as the increased activity of the antioxidant enzymes. In the MCAO model, the apoptosis rate of the dioscin-treated hippocampal neurons was attenuated compared with the MCAO group (P<0.05; Fig. 8H). In addition, HMGB-1 overexpression significantly increased neuronal apoptosis in rat hippocampus in the MCAO + dioscin + HMGB-1 group. These results suggested that dioscin may reverse the increased apoptosis rate via the HMGB-1 pathway.

Discussion

With high fatality and morbidity rates, cerebral ischemia not only seriously threatens patients' lives, but also increases the financial burden placed on families and society (28). An imbalance of energy supply and demand is caused by cerebral artery occlusion, which in turn leads to oxygen deficiency and glucose deprivation in the brain, ultimately resulting in neuronal injury (29). Following recovery of blood supply to the ischemic brain tissue, the excessive production of ROS may cause neuronal damage, which may result in more severe cellular dysfunction compared with hypoxia and ischemia only (30).

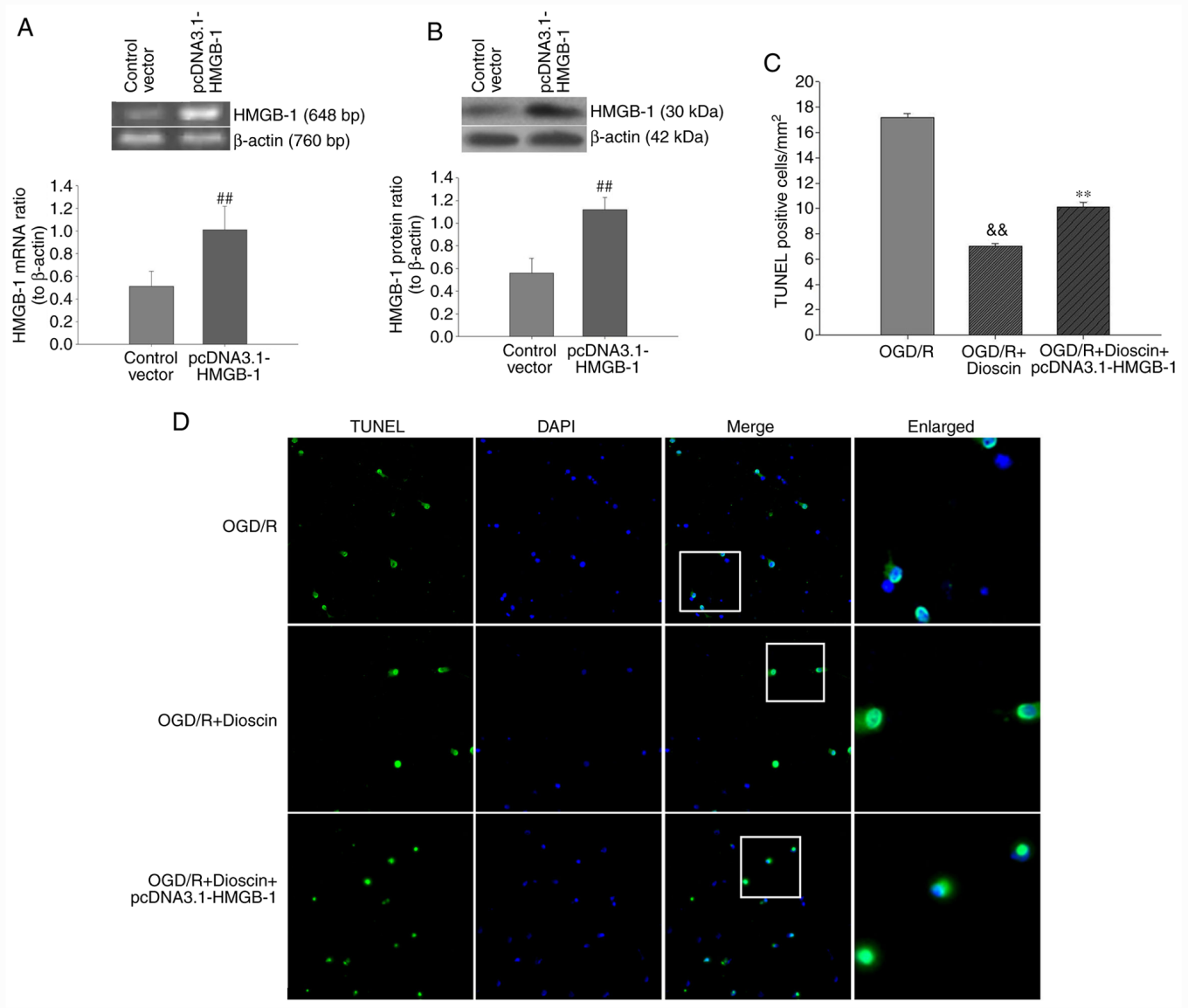

Figure 6. Effect of HMGB-1 overexpression on the apoptosis rate of primary hippocampal neurons following dioscin treatment. The transfection effect was confirmed by (A) PCR and (B) western blot analysis. ##P<0.01 vs. the control vector group. (C) Bar chart of TUNEL-positive cell ratios in different groups. Values are presented as means ± standard deviation (SD). **P<0.01 vs. the OGD/R group. (D) TUNEL-stained (green) cells indicate apoptosis-positive cells, DAPI stain (blue) indicates nucleated cells, and the 'merge' column shows cells stained with TUNEL and DAPI. Magnification, x200. White boxes represented magnified view of the typical apoptosis cells. Magnification, x400. &&P<0.01 vs. the OGD/R + dioscin group. HMGB-1, high mobility group box chromosomal protein 1; TUNEL, terminal deoxynucleotidyl transferase-mediated (dUTP) nick-end labeling; DAPI, 4',6-diamidino-2-phenylindole; OGD/R, oxygen-glucose deprivation/reperfusion.

The present study aimed to investigate the protective effects of dioscin in OGD/R-subjected neurons. The results indicated that dioscin exhibited antioxidative, anti-inflammatory, and antiapoptotic effects.

Dioscin, a compound with several pharmacological and biological activities, is a natural steroid saponin isolated from multiple plants (31). It has been reported that dioscin serves fundamental roles in several diseases, including refractory apical periodontitis, acute renal injury, and atherosclerosis (13,32,33). The possible mechanisms underlying its effects include anti-inflammatory, antioxidant stress and antiapoptotic activities. A previous study has demonstrated that oral feeding of dioscin for 7 consecutive days downregulated the mRNA expression levels of IL-1β, IL-6 and TNF-α in a hepatic IRI model (33). In addition, a recent study has suggested that disocin exerts its antioxidant effects not only via decreasing ROS production, but also by enhancing the activity of antioxidant enzymes (13). Furthermore, disocin mediates neuroprotection by suppressing inflammation and inhibiting the HMGB-1/toll-like receptor 4 (TLR4) pathway (34). These results were generally consistent with the observations of the present study in hippocampal neurons. Therefore, the results demonstrated that OGD/R-subjected neurons increased the protein and mRNA expression levels of IL-1β, IL-6 and TNF-α, concurrent with elevated ROS generation and an attenuated activity of antioxidative enzymes. Furthermore, treatment with dioscin (400 ng/ml) for 24 h remarkably improved neuron viability and decreased the expression of inflammatory cytokines. Subsequently, the balance of the oxidative and antioxidative system was also evaluated. Therefore, the

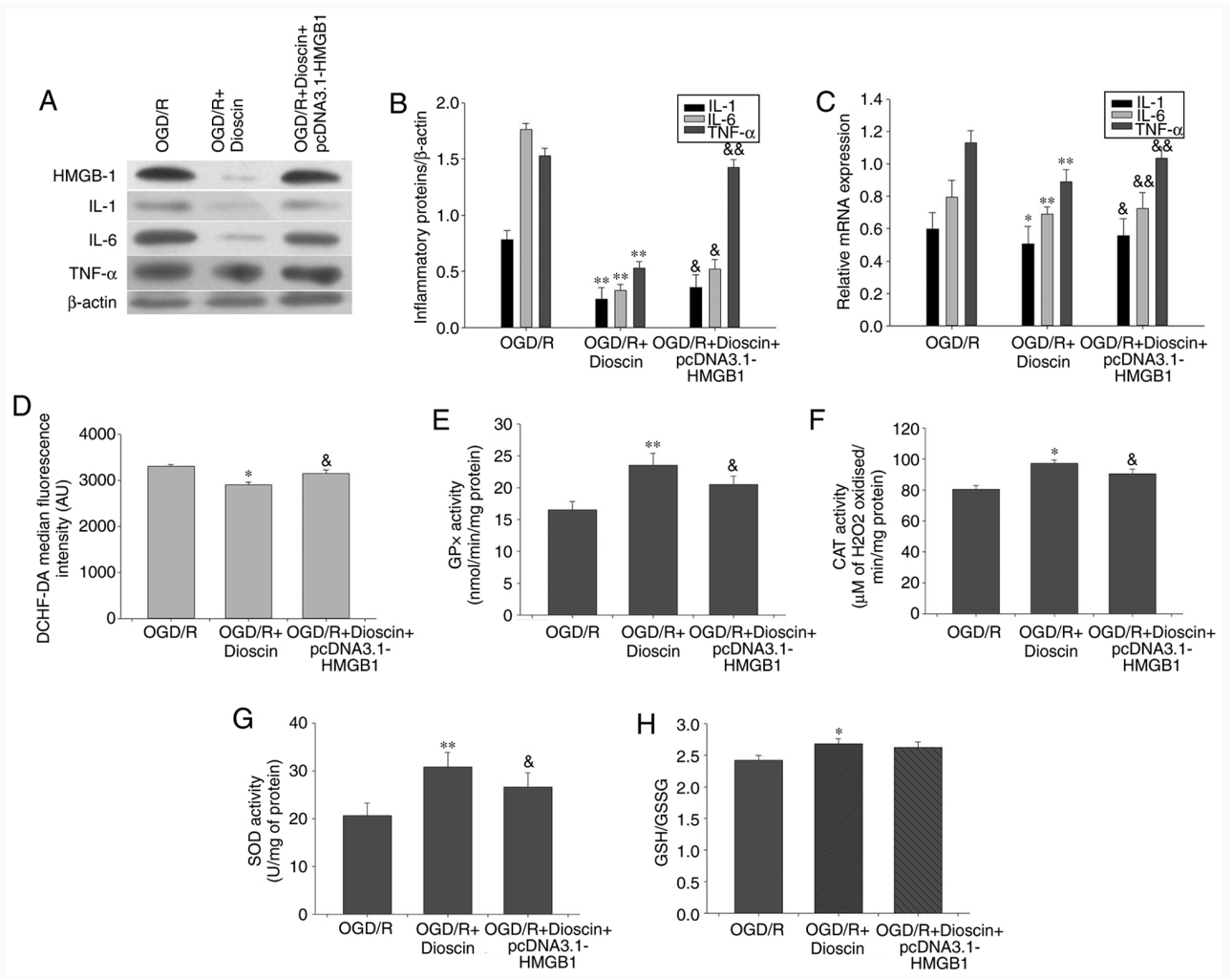

Figure 7. Inhibiting the activity of the HMGB-1/RAGE pathway reversed the effect of dioscin on the expression of proinflammatory cytokines, ROS generation and antioxidant stress. (A) Western blot analysis results showing IL-1, IL-6 and TNF-α protein expression. β-actin served as an internal control. (B) Bar chart showing the IL-1/β-actin, IL-6/β-actin and TNF-α/β-actin ratio from the western blot analysis results in different groups. (C) Bar chart showing IL-1/β-actin, IL-6/β-actin and TNF-α/β-actin ratio from RT-qPCR results in different groups. (D) DCHF-DA fluorescence intensity in different groups using flow cytometry. (E) GPx, (F) CAT and (G) SOD activity and (H) GSH/GSSG ratio in different groups. Values are presented as the means ± standard deviation (SD). *P<0.05 and **P<0.01 vs. the OGD/R group. $^{\&}$P<0.05 and $^{\&\&}$P<0.01 vs. the OGD/R + dioscin group. HMGB-1, high mobility group box chromosomal protein 1; RAGE, receptor for advanced glycation end products; ROS, reactive oxygen species; IL-1, interleukin 1; TNF-α, tumor necrosis factor α; DCHF-DA, 2',7'-dichlorofluorescein diacetate; GPx, glutathione peroxidase; CAT, catalase; SOD, superoxide dismutase; GSH/GSSG, glutathione/glutathione disulphide; OGD/R, oxygen-glucose deprivation/reperfusion.

activities of GPx, CAT and SOD, and the GSH/GSSG ratio were significantly elevated in dioscin-treated neurons. These results suggested that dioscin could exert neuroprotective effects, possibly mediated by its anti-inflammatory and antioxidative abilities.

Apart from its anti-inflammatory and antioxidant effects, the results of the current study revealed that dioscin attenuated neuron apoptosis via maintaining the homeostasis in the expression of the apoptosis-associated genes Bax and Bcl-2, as well as downregulating cleaved caspase-3 expression. These results were consistent with those obtained in the study by Tao *et al* in hepatic IRI (35). However, these results were different from those in other studies. Therefore, Zhang *et al* demonstrated that dioscin promoted cell apoptosis (36). Additionally, in hepatocellular carcinoma (HCC), dioscin significantly inhibited HCC cell proliferation and upregulated the expression of cleaved caspase-3 and Bax/Bcl-2. However, the possible mechanism underlying the effects of dioscin on neuronal survival remains unclear. Therefore, subsequent in-depth studies into its molecular mechanisms of action are required.

Regarding the exact mechanisms underlying the positive effects of dioscin, several studies have indicated that dioscin exerts its anti-inflammatory, antioxidative and antiapoptotic effects via the TLR4/myeloid differentiation factor 88 (MyD88) and peroxisome proliferator-activated receptor-γ coactivator-1α (PGC-1α)/estrogen receptor α (ERα) signaling pathways (13,37,38). As an important injury-associated compound, dioscin has been assumed to inhibit HMGB-1 in an IRI animal model (39). A previous study demonstrated that dioscin downregulated the expression of HMGB-1 and other inflammatory mediators, thus resulting in improving nerve injury caused by ischemia/hypoxia (35). HMGB-1 is considered as a crucial regulator in the early stages of organ ischemia-reperfusion

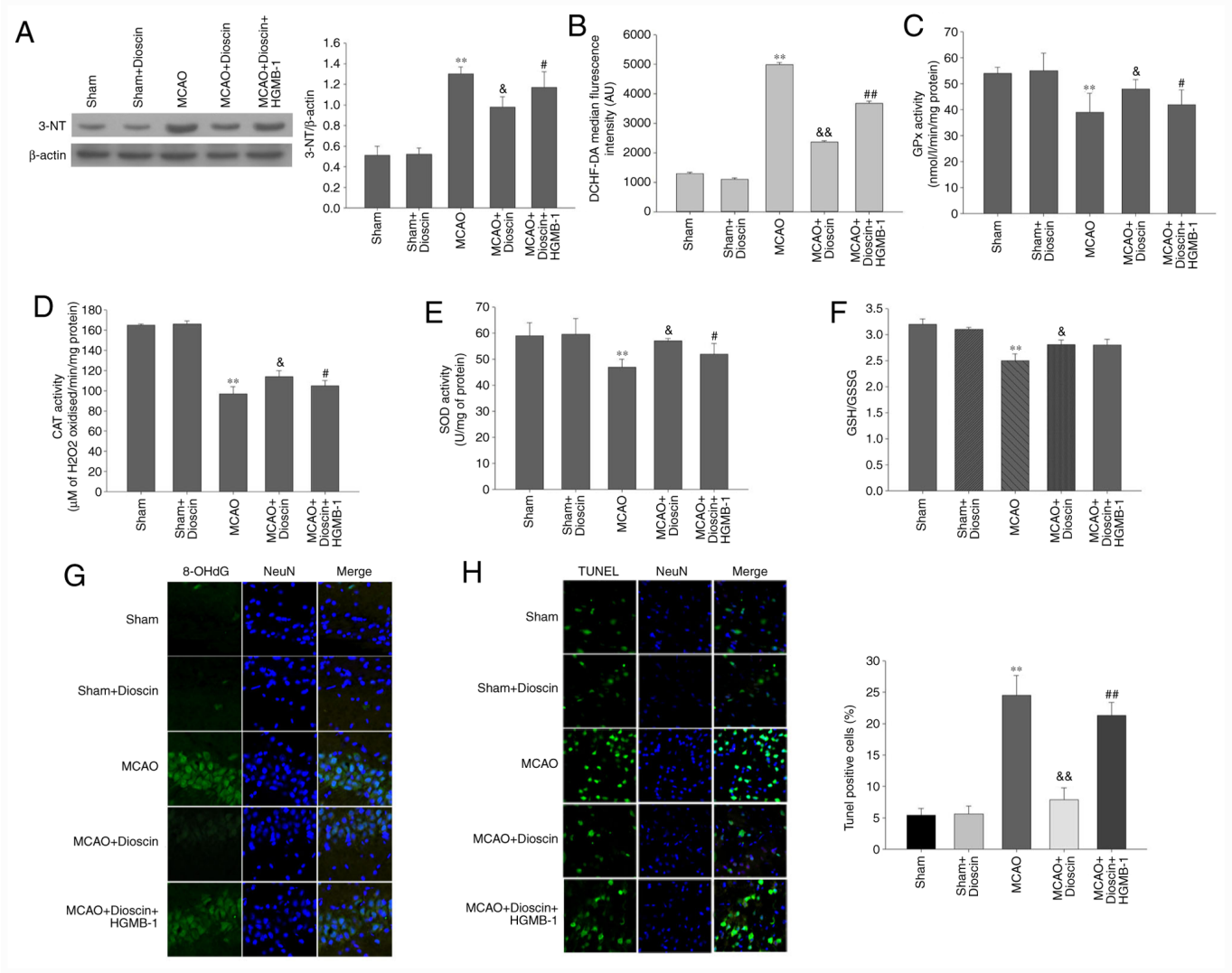

Figure 8. Dioscin remarkably alleviates oxidative stress and apoptosis of hippocampal neurons in the MCAO model via the HMGB-1/RAGE pathway. (A) The effect of dioscin and HMGB-1 on the expression of the 3-NT protein in rat hippocampal neurons. (B) DCHF-DA fluorescence intensity was quantified by flow cytometry. Dioscin improved the enzymatic antioxidant defenses in rat hippocampal neurons in the MCAO group via the HMGB-1 pathway. (C) GPx, (D) CAT and (E) SOD activities were evaluated in rat hippocampal neurons. Dioscin improved the non-enzymatic antioxidant defenses in rat hippocampal neurons of the MCAO group. This effect was not mediated via the HMGB-1 pathway. (F) The GSH/GSSG ratio was evaluated in rat hippocampal neurons of the MCAO group. (G) The effect of dioscin on the aggregation of the 8-OHdG protein in rat hippocampal neurons. 8-OHdG (green) was immunolabeled in rat hippocampal neurons. Magnification, x400. (H) Treatment with dioscin decreased the number of TUNEL-positive apoptotic cells in rat hippocampal tissue. Magnification, x200. Rat brain tissue sections were stained with TUNEL (green) and DAPI (blue). The bar chart shows the quantification of the TUNEL-positive cells (%). Values are expressed as the mean ± standard error of the mean (SEM). **P<0.01 vs. the sham group. $^{\&}$P<0.05 and $^{\&\&}$P<0.01 vs. the MCAO group. $^{\#}$P<0.05 and $^{\#\#}$P<0.01 vs. the MCAO + dioscin group. MCAO; middle cerebral artery occlusion; HMGB-1, high mobility group box chromosomal protein 1; RAGE, receptor for advanced glycation end products; DCHF-DA, 2',7'-dichlorofluorescein diacetate; GPx, glutathione peroxidase; CAT, catalase; SOD, superoxide dismutase; GSH/GSSG, glutathione/glutathione disulphide; 8-OHdG, 8-hydroxy-2'-deoxyguanosine; TUNEL, terminal deoxynucleotidyl transferase-mediated (dUTP) nick-end labeling; DAPI, 4',6-diamidino-2-phenylindole.

dysfunctions (40). It has been previously reported that HMGB-1 exerts a variety of cytoprotective activities combined with the downstream molecule RAGE (41). In the present study, dioscin suppressed the oxidative and inflammatory reactions, and attenuated OGD/R-associated apoptosis. During this process, the HMGB-1/RAGE signaling pathway was downregulated, thereby leading to a substantial decrease in the cell apoptosis rate, in order to maintain an adequate number of neurocytes. In addition, considerable changes in the intracellular ROS production and the activity of antioxidant enzymes were observed in the hippocampal neurons, probably mediated by the downregulation of the HMGB-1/RAGE pathway. However, there were no marked statistically significant differences in the GSH/GSSG ratios between the OGD/R + dioscin + pcDNA3.1-HMGB-1 and OGD/R + dioscin groups *in vivo*, as well as between the MCAO + dioscin and MCAO + dioscin + HMGB-1 groups *in vitro*. Furthermore, to the best of our knowledge, the association between the activation of the HMGB-1/RAGE pathway and non-enzymatic antioxidant defenses has not been previously investigated. This could be considered as another mechanism of dioscin action associated with its antioxidant effects, which requires further investigation. In addition to the TLR4/MyD88 and PGC-1α/ERα signaling pathways described above (13,37), numerous hypotheses have been formulated to explain the internal mechanism of dioscin resistance to OGD/R. As the neuroprotective effects of dioscin may involve

several mechanisms working together, a more comprehensive research base is required to investigate the potential mechanisms that may ensure the maintenance of neuronal function and survival.

In conclusion, treatment with dioscin decreased nerve injury and enhanced cell viability. These neuroprotective effects may primarily due to the maintenance of homeostasis in the antioxidative/oxidative system, as well as antiapoptotic and anti-inflammatory effects. Furthermore, the HMGB-1/RAGE signaling pathway was also determined to be involved in these processes. The results of the present study provided evidence in favor of considering dioscin as a promising neuroactive compound for ischemic stroke.

Acknowledgements

Not applicable.

Funding

No funding was received.

Availability of data and materials

All data generated or analyzed during this study are available from the corresponding author on reasonable request.

Authors' contributions

AL, WZ and JH were involved in the study design, and in the drafting and editing of the manuscript. AL, WZ, SW and YW performed the experiments. JH, SW and YW were involved in data interpretation. All authors have read and approved the final manuscript.

Ethics approval and consent to participate

This study was approved by the Animal Care and Use Committee, Tangshan Gongren Hospital, China (approval No. GRYY-LL-2019-15).

Patient consent for publication

Not applicable.

Competing interests

The authors declare that they have no competing interests.

References

1. Feigin V, Roth G, Naghavi M, Parmar P, Krishnamurthi R, Chugh S, Mensah GA, Norrving B, Shiue I, Ng M, *et al*: Global burden of stroke and risk factors in 188 countries, during 1990-2013: A systematic analysis for the Global Burden of Disease Study 2013. Lancet Neurol 15: 913-924, 2016.
2. Candelario-Jalil E: Injury and repair mechanisms in ischemic stroke: Considerations for the development of novel neurotherapeutics. Curr Opin Investig Drugs 10: 644-654, 2009.
3. Stoll G, Kleinschnitz C and Nieswandt B: Combating innate inflammation: A new paradigm for acute treatment of stroke? Ann N Y Acad Sci 1207: 149-154, 2010.
4. Scaffidi P, Misteli T and Bianchi ME: Release of chromatin protein HMGB1 by necrotic cells triggers inflammation. Nature 418: 191-195, 2002.
5. Zhang Z, Wu Y, Zhao Y, Xiao X, Liu J and Zhou X: Dynamic changes in HMGB1 levels correlate with inflammatory responses during cardiopulmonary bypass. Exp Ther Med 5: 1523-1527, 2013.
6. Tsung A, Sahai R, Tanaka H, Nakao A, Fink MP, Lotze MT, Yang H, Li J, Tracey KJ, Geller DA and Billiar TR: The nuclear factor HMGB1 mediates hepatic injury after murine liver ischemia-reperfusion. J Exp Med 201: 1135-1143, 2005.
7. Xie J, Méndez J D, Méndez-Valenzuela V and Aguilar-Hernández MM: Cellular signalling of the receptor for advanced glycation end products (RAGE). Cell Signal 25: 2185-2197, 2013.
8. Zhang F, Su X, Huang G, Xin XF, Cao EH, Shi Y and Song Y: sRAGE alleviates neutrophilic asthma by blocking HMGB1/RAGE signalling in airway dendritic cells. Sci Rep 7: 14268, 2017.
9. Jang HJ, Han IH, Kim YJ, Yamabe N, Lee D, Hwang GS, Oh M, Choi KC, Kim SN, Ham J, *et al*: Anticarcinogenic effects of products of heat-processed ginsenoside Re, a major constituent of ginseng berry, on human gastric cancer cells. J Agric Food Chem 62: 2830-2836, 2014.
10. Zhao X, Tao X, Xu L, Yin L, Qi Y, Xu Y, Han X and Peng J: Dioscin induces apoptosis in human cervical carcinoma HeLa and SiHa cells through ROS-mediated DNA damage and the mitochondrial signaling pathway. Molecules 21: 730, 2016.
11. Zhang Y, Xu Y, Qi Y, Xu L, Song S, Yin L, Tao X, Zhen Y, Han X, Ma X, *et al*: Protective effects of dioscin against doxorubicin-induced nephrotoxicity via adjusting FXR-mediated oxidative stress and inflammation. Toxicology 378: 53-64, 2017.
12. Ikeda T, Ando J, Miyazono A, Zhu XH, Tsumagari H, Nohara T, Yokomizo K and Uyeda M: Anti-herpes virus activity of Solanum steroidal glycosides. Biol Pharm Bull 23: 363-364, 2000.
13. Yang Q, Wang C, Jin Y, Ma X, Xie T, Wang J, Liu K and Sun H: Disocin prevents postmenopausal atherosclerosis in ovariectomized LDLR-/-mice through a PGC-1α/ERα pathway leading to promotion of autophagy and inhibition of oxidative stress, inflammation and apoptosis. Pharmacol Res 148: 104414, 2019.
14. Lu B, Yin L, Xu L and Peng J: Application of proteomic and bioinformatic techniques for studying the hepatoprotective effect of dioscin against CCl4-induced liver damage in mice. Planta Med 77: 407-415, 2011.
15. Lu J, Zhang T, Sun H, Wang S and Liu M: Protective effects of dioscin against cartilage destruction in a monosodium iodoacetate (MIA)-indcued osteoarthritis rat model. Biomed Pharmacother 108: 1029-1038, 2018.
16. Dias KL, Correia Nde A, Pereira KK, Barbosa-Filho JM, Cavalcante KV, Araújo IG, Silva DF, Guedes DN, Neto Mdos A, Bendhack LM and Medeiros IA: Mechanisms involved in the vasodilator effect induced by diosgenin in rat superior mesenteric artery. Eur J Pharmacol 574: 172-178, 2007.
17. Lee BK, Kim CJ, Shin MS and Cho YS: Diosgenin improves functional recovery from sciatic crushed nerve injury in rats. J Exerc Rehabil 14: 566-572, 2018.
18. Gong G, Qin Y and Huang W: Anti-thrombosis effect of diosgenin extract from *Dioscorea zingiberensis* CH Wright in vitro and in vivo. Phytomedicine 18: 458-463, 2011.
19. Zheng H, Wei Z, Xin G, Ji C, Wen L, Xia Q, Niu H and Huang W: Preventive effect of a novel diosgenin derivative on arterial and venous thrombosis in vivo. Bioorg Med Chem Lett 26: 3364-3369, 2016.
20. Liu J, Pasini S, Shelanski ML and Greene LA: Activating transcription factor 4 (ATF4) modulates post-synaptic development and dendritic spine morphology. Front Cell Neurosci 8: 177, 2014.
21. National Research Council (US) Institute for Laboratory Animal Research: Guide for the Care and Use of Laboratory Animals. National Academies Press, Washington, DC, 1996. https://www.ncbi.nlm.nih.gov/books/NBK232589/ doi: 10.17226/5140.
22. Xiong Y, Xia Y, Deng J, Yan X, Ke J, Zhan J, Zhang Z and Wang Y: Direct peritoneal resuscitation with pyruvate protects the spinal cord and induces autophagy via regulating PHD2 in a rat model of spinal cord ischemia-reperfusion injury. Oxid Med Cell Longev 2020: 4909103, 2020.
23. Livak KJ and Schmittgen TD: Analysis of relative gene expression data using real-time quantitative PCR and the 2(-Delta Delta C(T)) method. Methods 25: 402-408, 2001.
24. Hissin PJ and Hilf R: A fluorometric method for determination of oxidized and reduced glutathione in tissues. Anal Biochem 74: 214-226, 1976.

25. Flohé L and Günzler WA: Assays of glutathione peroxidase. Methods Enzymol 105: 114-121, 1984.
26. Aebi H: Catalase in vitro. Methods Enzymol 105: 121-126, 1984.
27. Hassan MQ, Akhtar MS, Akhtar M, Ansari SH, Ali J, Haque SE and Najmi AK: Benidipine prevents oxidative stress, inflammatory changes and apoptosis related myofibril damage in isoproterenol-induced myocardial infarction in rats. Toxicol Mech Methods 25: 26-33, 2015.
28. Hankey GJ: Stroke. Lancet 389: 641-654, 2017.
29. Onwuekwe IO and Ezeala-Adikaibe B: Ischemic stroke and neuroprotection. Ann Med Health Sci Res 2: 186-190, 2012.
30. Cuzzocrea S, Riley DP, Caputi AP and Salvemini D: Antioxidant therapy: A new pharmacological approach in shock, inflammation, and ischemia/reperfusion injury. Pharmacol Rev 53: 135-159, 2001.
31. Tao X, Yin L, Xu L and Peng J: Dioscin: A diverse acting natural compound with therapeutic potential in metabolic diseases, cancer, inflammation and infections. Pharmacol Res 137: 259-269, 2018.
32. Yin W, Liu S, Dong M, Liu Q, Shi C, Bai H, Wang Q, Yang X, Niu W and Wang L: A new NLRP3 inflammasome inhibitor, Dioscin, promotes osteogenesis. Small 16: e1905977, 2020.
33. Qi M, Zheng L, Qi Y, Han X, Xu Y, Xu L, Yin L, Wang C, Zhao Y, Sun H, *et al*: Dioscin attenuates renal ischemia/reperfusion injury by inhibiting the TLR4/MyD88 signaling pathway via up-regulation of HSP70. Pharmacol Res 100: 341-352, 2015.
34. Tao X, Sun X, Yin L, Han X, Xu L, Qi Y, Xu Y, Li H, Lin Y, Liu K and Peng J: Dioscin ameliorates cerebral ischemia/reperfusion injury through the downregulation of TLR4 signaling via HMGB-1 inhibition. Free Radic Biol Med 84: 103-115, 2015.
35. Tao X, Wan X, Xu Y, Xu L, Qi Y, Yin L, Han X, Lin Y and Peng J: Dioscin attenuates hepatic ischemia-reperfusion injury in rats through inhibition of oxidative-nitrative stress, inflammation and apoptosis. Transplantation 98: 604-611, 2014.
36. Zhang G, Zeng X, Zhang R, Liu J, Zhang W, Zhao Y, Zhang X, Wu Z, Tan Y, Wu Y and Du B: Dioscin suppresses hepatocellular carcinoma tumor growth by inducing apoptosis and regulation of TP53, BAX, BCL2 and cleaved CASP3. Phytomedicine 23: 1329-1336, 2016.
37. Yao H, Hu C, Yin L, Tao X, Xu L, Qi Y, Han X, Xu Y, Zhao Y, Wang C and Peng J: Dioscin reduces lipopolysaccharide-induced inflammatory liver injury via regulating TLR4/MyD88 signal pathway. Int Immunopharmacol 36: 132-141, 2016.
38. Zhang W, Yin L, Tao X, Xu L, Zheng L, Han X, Xu Y, Wang C and Peng J: Dioscin alleviates dimethylnitrosamine-induced acute liver injury through regulating apoptosis, oxidative stress and inflammation. Environ Toxicol Pharmacol 45: 193-201, 2016.
39. Zhu S, Tang S and Su F: Dioscin inhibits ischemic stroke-induced inflammation through inhibition of the TLR4/MyD88/NF-κB signaling pathway in a rat model. Mol Med Rep 17: 660-666, 2018.
40. Liu A, Dirsch O, Fang H, Sun J, Jin H, Dong W and Dahmen U: HMGB1 in ischemic and non-ischemic liver after selective warm ischemia/reperfusion in rat. Histochem Cell Biol 135: 443-452, 2011.
41. Bortolotto V and Grilli M: Every cloud has a silver lining: Proneurogenic effects of Aβ oligomers and HMGB-1 via activation of the RAGE-NF-κB axis. CNS Neurol Disord Drug Targets 16: 1066-1079, 2017.